

### A. $\text{Li}^6 + \text{Li}^6$

The spectrum appears in Fig. 1 and the data are summarized in Table I. Higher-gain spectra are reproduced here in Fig. 2 and are summarized in the appropriate tables.  $\text{C}^{11}$  and  $\text{Be}^7$  were detected with the beam off from the residual target radiation in amounts which give rough agreement with the yields for these reactions measured by Norbeck.<sup>3</sup> The neutrons responsible for excitation of levels in  $\text{I}^{127}$  and  $\text{Na}^{23}$  come from the reaction producing  $\text{C}^{11}$  and have energies up to 9 Mev.

### B. $\text{Li}^6 + \text{Li}^7$

The spectra appear in Figs. 1 and 2 and the data are summarized in Table II. The presence of  $\text{C}^{11}$  was again detected from the residual radiation with yields in rough agreement with Norbeck's measurements. The

<sup>3</sup> E. Norbeck, Jr., Phys. Rev. **121**, 824 (1961).

neutron sources are now  $\text{C}^{12} + n + 20.9$  Mev and  $\text{C}^{11} + 2n + 2.2$  Mev.

### C. $\text{Li}^7 + \text{Li}^7$

The spectra appear in Figs. 1 and 2 and the data are summarized in Table III. No residual radiation was detected. The neutron sources are  $\text{C}^{13} + n + 18.6$  Mev and  $\text{C}^{12} + 2n + 13.7$  Mev.  $\text{B}^{12}$  and  $\text{B}^{13}$  contribute a high-energy  $\beta$  spectrum.  $\text{B}^{13}$  has been observed from  $\text{Li}^7(\text{Li}^7, p)$  by Norbeck.<sup>1</sup> No evidence for  $\text{B}^{13}$  can be adduced from these data.

### ACKNOWLEDGMENTS

The author wishes to thank Professor R. R. Carlson, Professor E. Norbeck, and Professor S. Bashkin for their advice and many helpful discussions. The author also wishes to thank the staff of the Nuclear Physics group for their assistance.

## Isobaric States in Nonmirror Nuclei\*

J. D. ANDERSON, C. WONG, AND J. W. MCCLURE

*Lawrence Radiation Laboratory, University of California, Livermore, California*

(Received February 5, 1962)

The 14.8-Mev protons from the Livermore variable-energy cyclotron have been used to study  $(p, n)$  spectra from 13 selected target nuclei with mass numbers from 48 to 93 for a laboratory angle of  $23^\circ$ . Neutron energies were determined using standard time-of-flight techniques. All spectra show one strong neutron group at an energy corresponding in excitation in the final nucleus to the isobaric counterpart (analog state) of the target ground state, i.e., the  $Q$  value is the usual Coulomb energy displacement. The strong forward peaking of the angular distribution of the neutrons corresponding to the analog state in  $\text{V}^{51}(p, n)\text{Cr}^{51}$  confirms the direct nature of the reaction. Although it is tempting, on the basis of the narrow width of the isobaric states ( $< 300$  kev), to imply some validity to isotopic spin as a quantum number for masses up to  $A = 93$ , Lane and Soper have shown that isobaric states in adjoining nuclei can occur even in mass regions where isotopic spin is not a good quantum number.

### INTRODUCTION

MEASUREMENTS of neutron spectra emitted from  $(p, n)$  reactions in the energy region below 20 Mev have been carried out by several investigators.<sup>1-3</sup> Results of these measurements have been compared with theoretical calculations derived from the compound statistical model<sup>4</sup> of the nucleus. Direct reaction neutrons are observed as an excess of high-energy neutrons over that predicted by statistical models of the compound nucleus<sup>5</sup> and by the anisotropy (forward peaking) of the high-energy neutrons.<sup>2</sup> No structure was resolved in medium- $A$  nuclei because of poor counting statistics

and only gross features were observed. In the present experiment, standard time-of-flight techniques, together with an 8.7-m flight path, provided adequate energy resolution to resolve a prominent neutron group in all the observed neutron spectra.

The resolved neutron group is interpreted as being due to a direct reaction which leads to a particular final state of the residual nucleus, i.e., the isobaric counterpart of the target ground state. Evidence for the existence of an isobaric state in  $\text{Cr}^{51}$  from proton bombardment of  $\text{V}^{51}$  has been presented in a previous letter.<sup>5</sup> This reaction is assumed to go as follows: The incoming proton reacts with an  $f_{7/2}$  neutron, exchanges its charge, and is emitted as a neutron. In the initial state there are eight  $f_{7/2}$  neutrons available and three  $f_{7/2}$  protons. Since, by definition of an isobaric state, all the nuclear interactions within the initial and final nucleus are the same, the  $Q$  for the  $(p, n)$  reaction between  $\text{V}^{51}$  and its

\* Work was done under the auspices of the U. S. Atomic Energy Commission.

<sup>1</sup> P. C. Gugelot, Phys. Rev. **81**, 51 (1951).

<sup>2</sup> D. M. Thomson, Proc. Phys. Soc. (London) **A69**, 447 (1956).

<sup>3</sup> R. D. Albert, J. D. Anderson, and C. Wong, Phys. Rev. **120**, 2149 (1960).

<sup>4</sup> J. Blatt and V. F. Weisskopf, *Theoretical Nuclear Physics* (John Wiley & Sons, Inc., New York, 1952).

<sup>5</sup> J. D. Anderson and C. Wong, Phys. Rev. Letters **7**, 250 (1961).

isobaric state in  $\text{Cr}^{51}$  is the Coulomb energy displacement. Additional isobaric states have been identified from neutron spectra for the following target nuclei:  $\text{Ti}^{48}$ ,  $\text{V}^{51}$ ,  $\text{Cr}^{52}$ ,  $\text{Fe}^{56}$ ,  $\text{Co}^{59}$ ,  $\text{Ni}$ ,  $\text{Cu}^{63}$ ,  $\text{Cu}^{65}$ ,  $\text{Zn}$ ,  $\text{Ge}$ ,  $\text{Se}$ ,  $\text{Y}^{89}$ , and  $\text{Nb}^{93}$ .

## EXPERIMENTAL METHOD

### Geometry

The experimental geometry for measurements of neutron spectra is shown in Fig. 1(a). The detector located outside the target pit at 8.7 m from the self-supporting targets is well shielded from background produced at the Faraday cup, collimator, and beam sweeping slit.

The geometry for the angular distribution measurement is shown in Fig. 1(b). The collimators and beam stopper were made of carbon to minimize background neutron production. The tremendous flux of 4.4-Mev gamma rays produced by inelastic proton scattering, although it did not interfere with the neutron spectra, had to be reduced in order to insure proper functioning of the proton-electron discriminating circuit. The inclusion of lead shielding around the Faraday cup limited the minimum angle of observation to  $20^\circ$ . Measurements were made at 10 angles between  $20^\circ$  and  $90^\circ$  for an incident proton energy of 12.1 Mev.

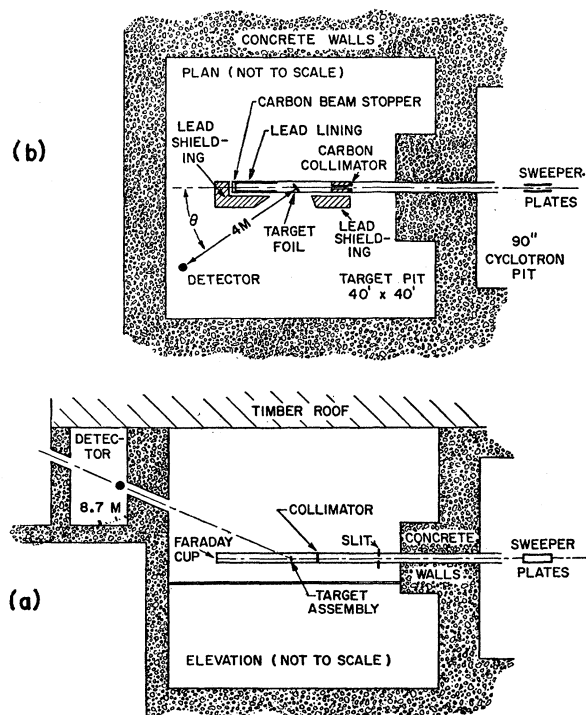


FIG. 1. Schematic diagram of the experimental geometry for (a) neutron spectra measurements, and (b) angular distribution measurements.

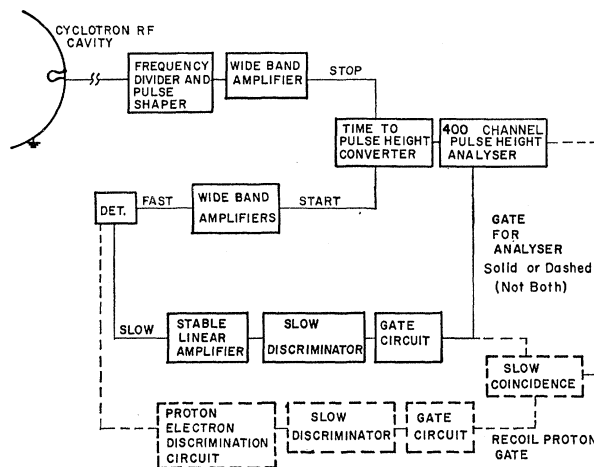


FIG. 2. Schematic diagram of the time-of-flight electronics. The dashed portion was added for the angular distribution measurement to suppress the gamma-ray background.

### Targets

Target thicknesses ranged from 150 to 300 kev. The V, Ni, and Nb were obtained commercially as foils. The Ti, Cr, Fe, Co, and Cu targets were evaporated and lifted as free films. The Zn and Ge were evaporated on 0.00025-in. gold backing, while the Se and Y were made as colloidal suspensions with a 0.0005-in. Mylar backing. Self-supporting targets are necessary to reduce the unwanted neutron production from the backing material.

### Electronics

A schematic diagram of the electronics is shown in Fig. 2. The solid portion of the diagram is conventional and has been described in a previous paper.<sup>6</sup> A 1-in. diameter by 1 in. long plastic scintillator and conventional electronics were used for all neutron spectra measurements. To increase the available time-of-flight and eliminate time overlap, three out of four pulses of protons from the cyclotron are swept off the target onto a tantalum slit [Fig. 1(a)]. Details of the beam-sweeping electronics and neutron time-of-flight instrumentation are given in a technical report.<sup>7</sup>

For the angular distribution measurements made inside the target pit, there was an appreciable gamma-ray background from the shielded collimator, the Faraday cup, and from neutron-capture gamma rays. To suppress the gamma radiation, a proton electron discrimination circuit was introduced as shown in the dashed portion of the Fig. 2 diagram. The discrimination circuit is used in conjunction with a 1- $\times$ 1-in. stilbene crystal.

<sup>6</sup> C. Wong, J. D. Anderson, C. Gardner, J. McClure, and M. P. Nakada, Phys. Rev. **116**, 164 (1959).

<sup>7</sup> J. D. Anderson and C. Wong, University of California Radiation Laboratory Report, UCRL-62927, 1961 (unpublished).

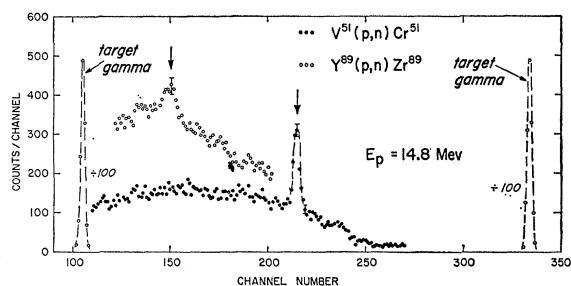


FIG. 3. Time-of-flight spectra from proton bombardment of V and Y. Time calibration of the system is 1.8 nsec/channel, and increasing time-of-flight is toward the left. The flight path was 8.7 m and the incident proton energy was 14.8 MeV.

### Results

The time-of-flight spectra resulting from 14.8-Mev proton bombardment of vanadium and yttrium are shown in Fig. 3. The target gamma ray appears twice, since a double display is used—one converter stop pulse for every two beam pulses. From Fig. 3 one sees that the principal background obscuring the neutrons corresponding to the isobaric state is “boil-off” neutrons from compound nucleus formation. The time-independent background (channel 260) is seen to be quite small. The energies of the neutron groups are calculated from their time of flight. The energy of the incident protons is determined by means of a differential range measurement in aluminum. As a check on systematic errors, the energies of neutrons produced in a thin aluminum target ( $\sim 80$  kev) were compared with the known excited states<sup>8</sup> as well as the ground-state<sup>9</sup>  $Q$  value. The data, corrected for target thickness and center-of-mass motion, are summarized in Table I. The  $Q$  values are also plotted in Fig. 4, together with the calculated

TABLE I. Experimental  $Q$  values (in Mev) for isobaric states.

	$E_p = 12.0$ Mev	$Q$ $E_p = 13.0$ Mev	$E_p = 14.8$ Mev
$Al^{27}(p,n)Si^{27}$			$5.53 \pm 0.08$
$Ti^{48}(p,n)V^{48}$			$7.91 \pm 0.10$
$V^{51}(p,n)Cr^{51}$	$8.0 \pm 0.2$	$8.04 \pm 0.15$	$8.05 \pm 0.10$
$Cr^{51}(p,n)Mn^{51}$		$8.38 \pm 0.15$	
$Fe^{56}(p,n)Co^{56}$	$8.9 \pm 0.2$	$8.79 \pm 0.15$	$8.73 \pm 0.13$
$Co^{59}(p,n)Ni^{59}$	$9.1 \pm 0.2$	$8.88 \pm 0.15$	$9.04 \pm 0.13$
$Ni(p,n)Cu$		$9.48 \pm 0.15$	$9.42 \pm 0.13$
$Cu^{63}(p,n)Zn^{63}$		$9.48 \pm 0.15$	$9.61 \pm 0.12$
$Cu^{65}(p,n)Zn^{65}$		$9.38 \pm 0.15$	$9.45 \pm 0.12$
$Zn(p,n)Ga$		$9.6$	$9.76 \pm 0.15$
$Ge(p,n)As$		$10.3$	$9.96 \pm 0.20$
$Se(p,n)Br$			$10.60 \pm 0.15$
$Y^{89}(p,n)Zr^{89}$			$11.60 \pm 0.15$
$Nb^{93}(p,n)Mo^{93}$			$11.90 \pm 0.15$

<sup>8</sup> S. Hinds and R. Middleton, Proc. Phys. Soc. (London) **73**, 727 (1959).

<sup>9</sup> D. A. Bromley, A. J. Ferguson, H. E. Gove, J. A. Kuehner, A. E. Litherland, E. Almquist, and R. Batchelor, Can. J. Phys. **37**, 1514 (1959).

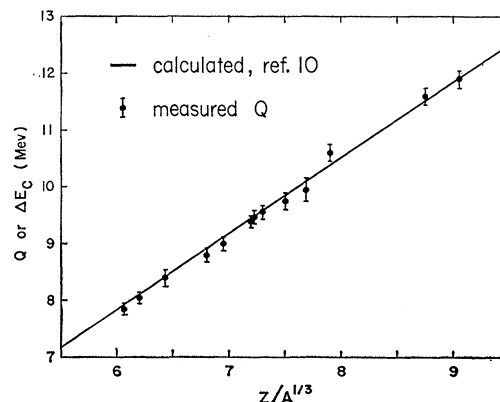


FIG. 4. Experimental  $Q$  values for isobaric states vs  $Z/A^{1/3}$ . The Coulomb displacement energy is calculated using  $r_0 = 1.27$  f.

Coulomb energies.<sup>10</sup> The agreement is seen to be very good.

Although a silver target was bombarded, no neutron group was observed. This is not surprising, however, since the computed ratio of the isobaric neutrons to the continuum neutrons is decreased a factor of 4 in going from Y to Ag. This is estimated from the nuclear temperatures and the relative neutron yields. Since the isobaric neutrons are only 15% of the continuum neutrons in Y, we would expect only a 4% effect in Ag and our statistics are not sufficiently good to detect such a small effect.

The angular distribution of the neutrons from the isobaric state in  $Cr^{51}$  was measured for a proton energy of 12.1 Mev. The data are plotted in Fig. 5. The errors are compounded from the statistical errors and the errors due to uncertainties in the line shape. As noted above, the principal background was due to continuum neutrons so it is necessary to use a line shape in order to extract the angular distribution data. This produces no appreciable error where the neutron group is prominent (near  $30^\circ$ ), but accounts for most of the error near  $90^\circ$ .

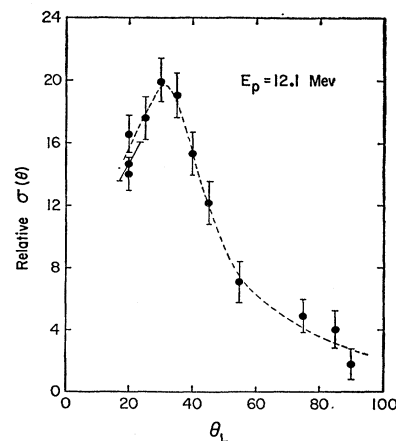


FIG. 5. Angular distributions of the neutrons from the analog state in  $V^{51}(p,n)Cr^{51}$ .

<sup>10</sup> N. Swamy and A. Green, Phys. Rev. **112**, 1719 (1958).

## CONCLUSIONS

## Angular Distributions

The strong forward peaking of the angular distribution of the neutrons corresponding to the analog state in  $V^{51}(p,n)Cr^{51}$  confirms the direct nature of the reaction.<sup>5</sup> The fact that the angular distribution shows no resemblance to the predictions of the plane-wave Born approximation (Butler theory)<sup>11</sup> is not surprising. In the low- $Z$  true mirror ( $p,n$ ) work, it has been shown<sup>12</sup> that, even as in ( $p,p'$ ) angular distributions, the nuclear distortion of ingoing and outgoing plane waves plays a dominant role in modifying the angular distributions. Using the Bloom formalism,<sup>13</sup> it may be possible to infer, from the angular distributions, information about two-body forces inside nuclear matter even in nonmirror nuclei.

## Coulomb Energy

Extensive use has been made of mirror-nuclei  $Q$  values to determine Coulomb energies.<sup>14</sup> The  $T=1$  nuclei<sup>15</sup> are included in the analysis by considering the change in Coulomb energy between the true mirror nuclei and the  $T=1$  nuclei as being due to a volume change only, caused by the addition or subtraction of one neutron. To compare our data with the mirror Coulomb energy, we follow the same procedure; we correct our measured Coulomb energy for the larger radii of our target nuclei caused by the neutron excess, assuming the volume is proportional to the number of nucleons, i.e.,  $E_c \text{ mirror} = E_c(A/A_{\text{mirror}})^{1/3}$ . The resultant mirror Coulomb energies are plotted in Fig. 6 along with other experimental data. The data derived from the ( $p,n$ ) reaction are not expected to show the shell effects which

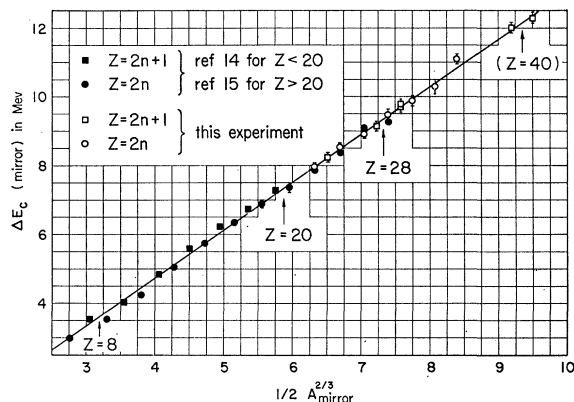


Fig. 6. Mirror Coulomb energies are plotted vs  $\frac{1}{2}A_{\text{mirror}}^{2/3}$ .

<sup>11</sup> S. T. Butler, Phys. Rev. **106**, 272 (1957).

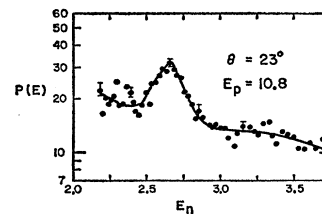
<sup>12</sup> C. Wong, J. D. Anderson, S. D. Bloom, J. W. McClure, and B. D. Walker, Phys. Rev. **123**, 598 (1961).

<sup>13</sup> S. D. Bloom, N. K. Glendenning, and S. A. Moszkowski, Phys. Rev. Letters **3**, 98 (1959); and S. D. Bloom (private communication).

<sup>14</sup> O. Kofoed-Hansen, Revs. Modern Phys. **30**, 449 (1958).

<sup>15</sup> J. H. Miller, III, Princeton thesis, Technical Report NYO-2959 (unpublished). We are indebted to Professor R. Sherr for bringing these data to our attention.

FIG. 7. Neutron energy spectrum from bombardment of an 8-mg/cm<sup>2</sup> V target with 10.8-Mev protons.



are prominently displayed by the true mirror-nuclei data<sup>14</sup> because all neutrons corresponding to unfilled proton shells can contribute, e.g., the Coulomb energy for  $Fe^{56}$  is averaged over  $2(f_{7/2})$  neutrons and  $2(2p_{3/2})$  neutrons. This same averaging process would tend to obscure any Coulomb pairing energy difference between proton pairs ( $Z=2n$  and  $Z=2n+1$ ). Although the accuracy of the present data limits its usefulness, it seems that, using the ( $p,n$ ) reaction, one may now accurately measure Coulomb displacement energies in the mass regions where no true mirror nuclides exist.

## Isotopic Spin

In Fig. 7 is plotted the neutron spectrum from the bombardment of an 8-mg/cm<sup>2</sup> V target with 10.8-Mev protons. The energy width of the target is approximately 200 keV. Since the width of the neutron group is less than 250 keV, it is clear that the width of the isobaric state is  $\leq 100$  keV. Although it is more difficult to accurately determine the width of the neutron group corresponding to  $Y^{89}$ , it is comparable to the target thickness and hence the width of the isobaric state is probably less than 300 keV. It is tempting on the basis of these small widths for the isobaric states to conclude that not only is  $\Delta T=0$ , but that isotopic spin is a good quantum number. Lane and Soper<sup>16</sup> have shown that, whereas all Coulomb forces contribute to isotopic spin mixing, the difference between isobaric states of neighboring nuclei arises from the Coulomb interaction of one proton only. Their calculations indicate that, even with appreciable isotopic spin mixing in the target nucleus, the width of the isobaric state near mass 93 is about the same as that of a pure isotopic spin state in light nuclei.

Additional experiments to more accurately determine the widths of the isobaric states as well as to improve the Coulomb energy measurements are in progress.

## ACKNOWLEDGMENTS

It is a pleasure to acknowledge the assistance of B. D. Walker in obtaining the data and Dr. H. Mark and Dr. S. D. Bloom for their comments regarding the interpretation of the data. Thanks are also due to Dr. Robert Jopson and the cyclotron crew under Donald Rawles for modifying the cyclotron such that we were able to obtain 15-Mev protons.

<sup>16</sup> A. M. Lane and J. M. Soper, Phys. Rev. Letters **7**, 420 (1961).